Journal of Organometallic Chemistry 880 (2019) 368–377

Contents lists available at ScienceDirect

Journal of Organometallic Chemistry

journal homepage: www.elsevier.com/locate/jorganchem

New insight into the reactions of organoplatinum(II) complexes with diorganotin dichloride and diisothiocyanate: Oxidative addition, reductive elimination and α-elimination☆

Badri Z. Momeni [a, *], Nastaran Fathi [a], Milad Moghadasi [a], Abbas Biglari [b], Jan Janczak [c]

[a] Faculty of Chemistry, K.N. Toosi University of Technology, P.O. Box 16315-1618, Tehran, 15418, Iran
[b] Department of Chemistry, Institute for Advanced Studies in Basic Sciences (IASBS), P.O. Box 451951159, Zanjan, Iran
[c] Institute of Low Temperature and Structure Research, Polish Academy of Sciences, P.O. Box 1410, 50-950, Wrocław 2, Poland

ARTICLE INFO

Article history:
Received 27 September 2018
Received in revised form
31 October 2018
Accepted 15 November 2018
Available online 29 November 2018

Keywords:
Organoplatinum
Organotin
Oxidative addition
Reductive elimination
NMR
Crystal structure

ABSTRACT

The reaction of electron rich [$PtMe_2$(NN)] with $SnMe_2Cl_2$ in a 1:3/Pt:Sn mole ratio resulted in formation of Pt(IV) complexes [$PtMe_2$($SnMe_2$Cl)Cl(NN)] {NN = 4,4′-Me_2bpy (4,4′-dimethyl-2,2′-bipyridine) (**7**); 5,5′-Me_2bpy (5,5′-dimethyl-2,2′-bipyridine) (**8**); bphen (4,7-diphenyl-1,10-phenanthroline) (**9**)}. NMR data show that the resulting complexes exist as the sole product corresponding to that of *trans* oxidative addition of $SnMe_2Cl_2$. The yellow polymorph of complex [$PtCl_2$(5,5′-Me_2bpy)] (**10**) was characterized by X-ray crystallography from the reaction of [$PtMe_2$(5,5′-Me_2bpy)] and excess of $SnMe_2Cl_2$ due to the reductive elimination of **8**. On the other hand, the reaction of [$PtMe_2$(NN)] with $SnEt_2Cl_2$ in a 1:3/Pt:Sn mole ratio resulted in formation of new complexes [$PtMe_2$($SnEt_2$Cl)Cl(4,4′-Me_2bpy)] (**11**), [$PtMe_2$($SnEt_2$Cl)Cl(5,5′-Me_2bpy)].$SnEt_2Cl_2$ (**12**) and [$PtMe_2$($SnEt_2$Cl)Cl(bu_2bpy)].$SnEt_2Cl_2$ (bu_2bpy = 4,4′-di-*tert*-butyl-2,2′-dipyridine) (**13**). NMR data indicate that the Pt—$SnEt_2$Cl bond is weaker than the Pt—$SnMe_2$Cl bond. The X-ray crystal structure of **13** reveals that organoplatinum(IV) complex acts as a donor to the $SnEt_2Cl_2$ to form an adduct in a distorted trigonal bipyramid with the axial Cl···Sn—Cl and equatorial $SnEt_2$Cl units. Moreover, the X-ray crystal structure of the new yellow form of [PtClMe(4,4′-Me_2bpy)] (**14**), which has been formed by the crystallization of a mixture of [$PtMe_2$(4,4′-Me_2bpy)] and excess of $SnEt_2Cl_2$, is described. The reaction of dimethylplatinum(II) complexes with dimethyltin diisothiocanate are reported for the first time which occur *via* Sn-NCS bond cleavage to afford the organoplatinum(IV) complexes [$PtMe_2$($SnMe_2$NCS)(SCN)(NN)] {NN = bpy (**17**); phen (**18**); 5,5′-Me_2bpy (**19**); bu_2bpy (**20**); bphen (**21**)}. The crystal structures of the novel thiocyanatoplatinum(IV) complexes [$PtMe_2$($SCN)_2$(bpy)] (**22**) and [$PtMe_2$($SCN)_2$(5,5′-Me_2bpy)]. H_2O (**23**) are discussed which have been obtained due to the α-elimination of $SnMe_2$. The crystal structures of **22**—**23** show that platinum adopts a slightly distorted octahedral geometry with *trans*- Pt($SCN)_2$ configuration in which SCN is bonded through sulfur atom while the nitrogen atom is coordinated to tin. NMR data indicate that the products dissociate *via* α-elimination of $SnMe_2$ or reductive elimination of organotin(IV) compound and the stability of the organoplatinum(IV) compounds varies according to the trends [$PtMe_2$($SnMe_2$Cl)Cl(NN)]>[$PtMe_2$($SnMe_2$NCS)(SCN)(NN)]>[$PtMe_2$($SnEt_2$Cl)Cl(NN)].

1. Introduction

Oxidative addition reactions have attracted growing attention due to the particular importance in catalytic chemistry, supramolecular chemistry, and platinum based drugs [1–4]. Among them, the oxidative addition reactions of organoplatinum(II) are of particular interest and a variety of Pt(IV) complexes were synthesized *via* activation of HX, C-X, Sn-X, Ge-X, Hg-X and Au-X bonds (X = halide) [5–15]. One of the most versatile organometallic reagents is organotin compounds which are particularly important in many catalyzed reactions in organic chemistry such as Stille reaction, palladium-catalyzed cross coupling of organostannates and

☆ This paper is in honor of Professor Richard J. Puddephatt, Pioneer of Oxidative Addition Reactions in Organoplatinum Chemistry, on the occasion of his 75th birthday.

* Corresponding author.
E-mail address: momeni@kntu.ac.ir (B.Z. Momeni).

https://doi.org/10.1016/j.jorganchem.2018.11.022
0022-328X/

organic electrophiles [16,17]. Despite the importance of binary mixtures of Pt(II)/Sn(II) compounds in several catalytic reactions such as hydrogenation and hydroformylation of olefins, few have been isolated [18–23]. The reactions of organoplatinum(II) complexes with tin halides generally can be divided to two main reactions: oxidative addition of Sn^{IV}-X bond (X = halide) to dimethylplatinum(II) complexes and the insertion of Sn^{II}-X into $Pt^{II/IV}$-X bond [24–30]. However, the exchange of halide can be observed in the case of mixed halide systems [31,32]. Remarkably, the reaction of dimethylplatinum(II) complexes with organotin halides can be as an equilibrium between parent Pt(II) complex and the resulting Pt(IV) product or self-association between halide ion as a donor and organotin(IV) halide as the acceptor [13,33–35].

Oxidative addition of Sn^{IV}-X bonds is one of the most complicate reactions among the group(IV)-X activation due to the competitive reactions such as reductive elimination in the case of diimine or phosphine ligands or the formation of an adduct between the second organotin(IV) compound and halide of the Pt-X bond [24,34–36]. Interestingly, we have previously reported that the dissociation of *trans*-[$PtMe_2(CH_2Cl)(phen)(PPh_3)$][$SnCl_3$].$C_2Cl_2H_4$ in solution results in the formation of [$SnCl_4$(phen)] [37]. In earlier report, we have reported that [$PtBr_2$(bpy)] was formed during the crystallization of *cis*- and *trans*-[$PtMe_2(SnBr_2Cl)(CH_2Cl)$(bpy)] [31]. In addition, the selective cleavage of Pt–Me bond was achieved in the case of reaction of dimethylplatinum(II) containing chelating phosphine ligands with $SnMe_2Cl_2$ and $SnPh_3Cl$ which was assigned to the presence of strong π-acceptor phosphine ligands [36]. The thermal stability of *trans*-[$PtMe_2(SnMe_3)Cl$(bpy)] indicates that three composition pathway are possible; competitive reductive elimination of $SnMe_3Cl$, $SnMe_4$ and elimination of $SnMe_2$ [38].

As an extension to our ongoing interest in the synthesis of the binary mixtures of platinum and tin complexes, we present here new insight into the reaction of diimine organoplatinum(II) compounds with diorganotin dichloride or diisothiocyanate. These are also the first examples of activation of Sn-isothiocyanate bond and $SnEt_2Cl_2$ to dimethylplatinum(IV) complexes. Accordingly, the novel stable dithiocyanatoplatinum(IV) complexes have been prepared in this way.

2. Experimental

2.1. General remarks

All reagents and solvents commercially available (Alpha Aesar, Sigma Aldrich, Acros, Merck) and were used without further purification. Elemental analyses were performed by a Flash EA 1112 elemental analyzer. The ^{1}H, ^{13}C, ^{119}Sn, ^{195}Pt, HH-COSY, HSQC and DEPT-135° NMR spectra were recorded using Biospin GmbH 400 spectrometer using residual solvent peaks, Na_2PtCl_6 (^{195}Pt) and $SnMe_4$ (^{119}Sn) as references. All the chemical shifts and coupling constants are reported in ppm and Hz, respectively. The UV–Vis study was performed using a single beam Camspect M330 UV/visible spectrophotometer at room temperature. IR spectra in the 4000-400 cm^{-1} were recorded on KBr pellets using ABB Bomem Model FTLA200-100 spectrophotometer. The starting complexes [$Pt_2Me_4(\mu\text{-}SMe_2)_2$], [$PtMe_2$(bpy)] (**1**), [$PtMe_2$(phen)] (**2**), [$PtMe_2$(4,4′-$Me_2$bpy)] (**3**), [$PtMe_2$(5,5′-$Me_2$bpy)] (**4**), [$PtMe_2$(-$bu_2$bpy)] (**5**) and [$SnMe_2(NCS)_2$] were prepared according to the literature [39–43]. The numerical data for NMR spectroscopy are summarized in the Experimental Section and NMR spectra are provided in Supplementary Information (Figs. S1–S9).

2.2. Preparation of [$PtMe_2$(bphen)] (**6**)

To a solution of [$Pt_2Me_4(\mu\text{-}SMe_2)_2$] (51 mg, 0.09 mmol) in acetone (5 mL) was added a solution of bphen (59 mg, 0.18 mmol) in acetone (30 mL). The reaction color changed to deep red and the solution stirred for 2 h at room temperature. After removal of the solvent under reduced pressure, the dark red complex was obtained and air dried. Yield: 72%; m.p. 221 °C (dec). Anal. Calc. for $C_{26}H_{22}N_2Pt$: C, 56.01; H, 3.98; N, 5.02. Found: C, 55.67; H, 4.27; N, 4.77%. NMR data in $CDCl_3$: $\delta(^1H)$ 1.30 [s, 6H, ^2J(Pt–H) = 85.3 Hz, Pt–Me], 7.56 [s, 10H, Ph groups], 7.75 [d, 2H, ^3J(HH) = 5.1 Hz, H^3], 7.94 [s, 2H, H^5], 9.56 [d, 2H, ^3J(HH) = 5.1 Hz, ^3J(Pt–H) = 25.4 Hz, H^2]; $\delta(^{13}C)$ −17.1 [s, ^1J(Pt–C) = 804 Hz, Pt–Me], 125.2 (C^5), 126.1 [C^3, ^2J(Pt–C) = 19 Hz], 128.8 (C^1), 129.2–129.4 (Ph groups), 137.1 (C^{13}), 146.4 [C^2, ^2J(Pt–C) = 33 Hz], 148.6 (C^{11}), 148.8 (C^4); $\delta(^{195}Pt)$ −3359. UV–Vis (λ_{max} in toluene): 474 and 516 nm.

2.3. Preparation of [$PtMe_2(SnMe_2Cl)Cl$(4,4′-Me_2bpy)] (**7**)

To a stirred solution of [$PtMe_2$(4,4′-Me_2bpy)] (66 mg, 0.16 mmol) in CH_2Cl_2 (3 mL) was added $SnMe_2Cl_2$ (106 mg, 0.48 mmol). The solution color was changed immediately from orange to pale yellow. After 10 min, 30 mL of diethyl ether/pentane (1:1) was added to precipitate the product as a pale yellow solid, which was isolated by filtration, washed with diethyl ether and air dried. Yield: 55%; m.p. 190–192 °C. Anal. Calc. for $C_{16}H_{24}Cl_2N_2PtSn$: C, 30.55; H, 3.85; N, 4.45. Found: C, 30.84; H, 3.98; N, 5.27%. NMR data in $CDCl_3$: $\delta(^1H)$ 0.38 [s, 6H, $^2J(^{119/117}Sn–H)$ = 47.9 Hz, Sn–Me], 1.33 [s, 6H, ^2J(Pt–H) = 55.7 Hz, Pt–Me], 2.53 [s, 6H, CH_3 of 4,4′-Me_2bpy], 7.42 [d, 2H, ^3J(HH) = 5.1 Hz, H^5], 8.06 [s, 2H, H^3], 8.71 [d, 2H, ^3J(HH) = 5.9 Hz, ^3J(Pt–H) = 19.3 Hz, H^6]; $\delta(^{13}C)$ −12.4 [s, ^1J(Pt–C) = 569 Hz, Pt–Me], −3.5 [s, $^1J(^{119/117}Sn–C)$ = 297, ^2J(Pt–C) = 98 Hz, Sn–Me], 21.8 [s, CH_3 of 4,4′-Me_2bpy], 124.6 (C^3), 127.7 (C^5), 147.0 (C^6), 151.4 (C^4), 155.3 (C^2); $\delta(^{119}Sn)$ 17 [s, ^1J(Pt–Sn) = 12964 Hz]; $\delta(^{195}Pt)$ −2884 [s, ^1J(Pt–^{119}Sn) = 13082 Hz, ^1J(Pt–^{117}Sn) = 12422 Hz].

2.4. Preparation of [$PtMe_2(SnMe_2Cl)Cl$(5,5′-Me_2bpy)] (**8**)

Following the same procedure as the synthesis of **7**, the reaction of [$PtMe_2$(5,5′-Me_2bpy)] (70 mg, 0.17 mmol) with $SnMe_2Cl_2$ (113 mg, 0.51 mmol) gave a pale yellow solid. Yield: 58%; m.p. 187 °C (dec). Anal. Calc. for $C_{16}H_{24}Cl_2N_2PtSn$: C, 30.55; H, 3.85; N, 4.45. Found: C, 30.35; H, 4.11; N, 5.38%. NMR data in $CDCl_3$: $\delta(^1H)$ 0.35 [s, 6H, $^2J(^{119/117}Sn–H)$ = 48.9 Hz, Sn–Me], 1.35 [s, 6H, ^2J(Pt–H) = 55.7 Hz, Pt–Me], 2.40 [s, 6H, CH_3 of 5,5′-Me_2bpy], 7.80 [br d, 2H, ^3J(HH) = 8.1 Hz, H^3], 8.06 [s, 2H, ^3J(HH) = 8.3 Hz, H^4], 8.65 [br s, 2H, ^3J(Pt–H) = 15.6 Hz, H^6]; $\delta(^{13}C)$ −12.0 [s, ^1J(Pt–C) = 569 Hz, Pt–Me], −3.6 [s, $^1J(^{119/117}Sn–C)$ = 299 Hz, ^2J(Pt–C) = 100 Hz, Sn–Me], 18.9 [s, CH_3 of 5,5′-Me_2bpy], 123.0 (C^4), 137.3 (C^5), 139.7 (C^3), 147.7 (C^6), 153.1 (C^2); $\delta(^{119}Sn)$ −116, −62, −31, 19 [s, ^1J(Pt–Sn) = 12900 Hz]; $\delta(^{195}Pt)$ −2886 [s, ^1J(Pt–^{119}Sn) = 12963 Hz, ^1J(Pt–^{117}Sn) = 12360 Hz]. Yellow crystals of [$PtCl_2$(5,5′-Me_2bpy)] (**10**) suitable for single crystal X-ray structure determination were grown from a mixture of an acetone solution of [$PtMe_2$(5,5′-Me_2bpy)] and $SnMe_2Cl_2$ in a 1:4 mol ratio during 3 days.

2.5. Preparation of [$PtMe_2(SnMe_2Cl)Cl$(bphen)] (**9**)

Similarly, the reaction of [$PtMe_2$(bpen)] (45 mg, 0.08 mmol) with $SnMe_2Cl_2$ (53 mg, 0.24 mmol) gave a yellow solid. Yield: 68%; m.p. 205–207 °C. Anal. Calc. for $C_{28}H_{28}Cl_2N_2PtSn$: C, 43.27; H, 3.63; N, 3.60. Found: C, 43.40; H, 3.95; N, 4.31%. NMR data in $CDCl_3$: $\delta(^1H)$ 0.41 [s, 6H, $^2J(^{119/117}Sn–H)$ = 48.7 Hz, Sn–Me], 1.55 [s, 6H, ^2J(Pt–H) = 55.7 Hz, Pt–Me], 7.54–7.60 [m, 10H, Ph groups], 7.90 [d, 2H, ^3J(HH) = 5.1 Hz, H^3], 8.05 [s, 2H, H^5], 9.26 [d, 2H, ^3J(HH) = 5.4 Hz, ^3J(Pt–H) = 20.5 Hz, H^2]; $\delta(^{13}C)$ −12.4 [s, ^1J(Pt–C) = 570 Hz, Pt–Me], −3.4 [s, $^1J(^{119/117}Sn–C)$ = 300 Hz, ^2J(Pt–C) = 100 Hz, Sn–Me], 125.8 (C^5), 126.0 (C^3), 129.3–129.9 (Ph

groups), 136.0 (C^{13}), 147.3 [C^2, ^2J(Pt–C) = 19 Hz], 147.6 (C^{11}), 151.5 (C^4); $\delta(^{119}Sn)$ 19 [s, ^1J(Pt–Sn) = 12878]; $\delta(^{195}Pt)$ −2918 [s, ^1J(Pt-$^{119/117}$Sn) = 12947 Hz].

2.6. Preparation of [$PtMe_2(SnEt_2Cl)Cl(4,4'\text{-}Me_2bpy)$] (**11**)

Similarly, the reaction of [$PtMe_2(4,4'\text{-}Me_2bpy)$] (65 mg, 0.16 mmol) with $SnEt_2Cl_2$ (118 mg, 0.48 mmol) gave a pale yellow solid. Yield: 50%; m.p. 191–193 °C. Anal. Calc. for $C_{18}H_{28}Cl_2N_2PtSn$. 0.5acetone: C, 34.13; H, 4.55; N, 4.08. Found: C, 34.33; H, 4.39; N, 4.96%. NMR data in $CDCl_3$: $\delta(^1H)$ 1.02 [m, 6H, CH_3 of Et], 1.08 [m, 4H, $^2J(^{119/117}Sn–H)$ = not resolved, PtCH_2], 1.36 [s, 6H, ^2J(Pt–H) = 55.7 Hz, Pt–Me], 2.51 [s, 6H, CH_3 of 4,4′-Me_2bpy], 7.40 [d, 2H, ^3J(HH) = 5.1 Hz, H^5], 8.06 [s, 2H, H^3], 8.71 [d, 2H, ^3J(HH) = 5.6 Hz, ^3J(Pt–H) = 20.3 Hz, $H^{6'}$]; $\delta(^{13}C)$ −13.7 [s, ^1J(Pt–C) = 570 Hz, Pt–Me], 8.2 [s, $^1J(^{119/117}Sn–C)$ = 297 Hz, ^2J(Pt–C) = 98 Hz, SnCH_2], 10.3 [s, $^2J(^{119/117}Sn–C)$ = not resolved, ^3J(Pt–C) = 27 Hz, CH_3 of Et], 21.8 [s, CH_3 of 4,4′-Me_2bpy], 124.6 (C^3), 127.6 (C^5), 147.1 [s, ^2J(Pt–C) = not resolved, $^3J(^{119/117}Sn–C)$ = 18 Hz, C^6], 151.4 (C^4), 155.3 (C^2); $\delta(^{119}Sn)$ 25 [s, ^1J(Pt–Sn) = 11595 Hz]; $\delta(^{195}Pt)$ −2838 [s, ^1J(Pt–^{119}Sn) = 11590 Hz, ^1J(Pt–^{117}Sn) = 11090 Hz]. Yellow single crystals of [PtMeCl(4,4′-Me_2bpy)] (**14**) were grown by slow evaporation a mixture of an acetone solution of [$PtMe_2(4,4'\text{-}Me_2bpy$)] and excess of $SnEt_2Cl_2$ at room temperature.

2.7. Preparation of [$PtMe_2(SnEt_2Cl)Cl(5,5'\text{-}Me_2bpy)$].$SnEt_2Cl_2$ (**12**)

Similarly, the reaction of [$PtMe_2(5,5'\text{-}Me_2bpy$)] (61 mg, 0.15 mmol) with $SnEt_2Cl_2$ (111 mg, 0.45 mmol) gave a pale yellow solid. Yield: 49%; m.p. 156–158 °C. Anal. Calc. for $C_{18}H_{28}Cl_2N_2PtSn.SnEt_2Cl_2$: C, 29.20; H, 4.23; N, 3.10. Found: C, 29.34; H, 4.53; N, 3.02%. NMR data in $CDCl_3$: $\delta(^1H)$ 1.03 [m, 6H, CH_3 of Et], 1.07 [m, 4H, $^2J(^{119/117}Sn–H)$ = not resolved, PtCH_2], 1.38 [s, 6H, ^2J(Pt–H) = 54.5 Hz, Pt–Me], 1.41 [m, CH_3 of free $SnEt_2Cl_2$], 1.72 [m, CH_2 of free $SnEt_2Cl_2$], 2.50 [s, 6H, CH_3 of 5,5′-Me_2bpy], 7.84 [d, 2H, ^3J(HH) = 7.8 Hz, H^3], 8.07 [d, 2H, ^3J(HH) = 8.1 Hz, H^4], 8.67 [s, 2H, ^3J(Pt–H) = 16.2 Hz, H^6]; $\delta(^{13}C)$ −13.2 [s, ^1J(Pt–C) = 572 Hz, Pt–Me], 8.4 [s, $^1J(^{119/117}Sn–C)$ = not resolved, ^2J(Pt–C) = 100 Hz, SnCH_2], 9.5 [s, CH_3 of Et], 10.0 [CH_3 of free $SnEt_2Cl_2$], 18.9 [s, CH_3 of 5,5′-Me_2bpy], 19.9 [CH_2 of free $SnEt_2Cl_2$], 122.9 (C^4), 137.4 (C^5), 139.7 (C^3), 148.0 (C^6), 153.3 (C^2); $\delta(^{119}Sn)$ 28 [s, ^1J(Pt–Sn) = 11446 Hz], 96; $\delta(^{195}Pt)$ −2833 [s, ^1J(Pt–^{119}Sn) = 11590 Hz, ^1J(Pt–^{117}Sn) = 11132 Hz]. The crystallization of **12** from DMSO led to the formation of light yellow crystals of [$Sn_4Et_8Cl_2O_2(OH)_2$] (**15**), suitable for X-ray crystallographic study.

2.8. Preparation of [$PtMe_2(SnEt_2Cl)Cl(bu_2bpy)$].$SnEt_2Cl_2$ (**13**)

Similarly, the reaction of [$PtMe_2(bu_2bpy$)] (40 mg, 0.08 mmol) with $SnEt_2Cl_2$ (60 mg, 0.24 mmol) gave a pale yellow solid. Yield: 67%; m.p. 308–311 °C (dec.). Anal. Calc. for $C_{24}H_{40}Cl_2N_2PtSn.SnEt_2Cl_2$: C, 34.00; H, 5.10; N, 2.83. Found: C, 34.66; H, 5.38; N, 2.85%. NMR data in $CDCl_3$: $\delta(^1H)$ 1.03 [m, 6H, CH_3 of Et], 1.11 [m, 4H, $^2J(^{119/117}Sn–H)$ = not resolved, PtCH_2], 1.35 [s, 6H, ^2J(Pt–H) = 54.8 Hz, Pt–Me], 1.42 [m, CH_3 of free $SnEt_2Cl_2$], 1.44 [s, 6H, CH_3 of bu_2bpy], 1.71 [m, CH_2 of free $SnEt_2Cl_2$], 7.62 [dd, 2H, ^3J(HH) = 5.9 Hz, ^4J(HH) = 1.5 Hz, H^5], 8.13 [d, 2H, ^4J(HH) = 1.7 Hz, H^3], 8.78 [d, 2H, ^3J(HH) = 5.9 Hz, ^3J(Pt–H) = 20.8 Hz, H^6]; $\delta(^{13}C)$ −13.6 [s, ^1J(Pt–C) = 569 Hz, Pt–Me], 8.5 [s, $^1J(^{119/117}Sn–C)$ = not resolved, ^2J(Pt–C) = 95 Hz, SnCH_2], 9.5 [s, CH_3 of Et], 10.0 [CH_3 of free $SnEt_2Cl_2$], 21.1 [CH_2 of free $SnEt_2Cl_2$], 30.5 (s, terminal C of ^{t}Bu), 35.7 (s, central C of ^{t}Bu), 120.3 (C^3), 124.3 (C^5), 147.4 (C^6), 155.6 (C^4), 164.1 (C^2); $\delta(^{119}Sn)$ −139, −91, 25 [s, ^1J(Pt–Sn) = 11526 Hz], 95; $\delta(^{195}Pt)$ −2838 [s, ^1J(Pt-$^{119/117}$Sn) = 11686 Hz]. The needle yellow single crystals of [$PtMe_2(SnEt_2Cl)Cl(bu_2bpy)$]. $SnEt_2Cl_2$ were grown from evaporation of a dichloromethane solution of **13** at room temperature after 3 days. Crystallization of **13** from dichloromethane/n-pentane at 4 °C gave crystals of yellow solid [$PtCl_2(bu_2bpy)$] (**16**) after 1 week.

2.9. Preparation of [$PtMe_2(SnMe_2NCS)(SCN)(bpy)$] (**17**)

To a solution of [$PtMe_2(bpy)$] (120 mg, 0.31 mmol) in acetone (15 mL) was added a solution of $SnMe_2(SCN)_2$ (83 mg, 0.31 mmol) in acetone (5 mL). The mixture was stirred for 24 h at the room temperature, during which time the product formed as a pale yellow precipitate. The mixture was filtered and the precipitate was washed with diethyl ether and air dried. Yield: 68%; m.p. 193–195 °C. Anal. Calc. for $C_{16}H_{20}N_4PtS_2Sn$: C, 29.74; H, 3.12; N, 8.67; S, 9.92. Found: C, 30.21; H, 3.25; N, 8.09; S, 9.30%. Selected IR data (KBr, cm^{-1}): 3004–2817 (C–H), 2104 (SCN), 2051 (NCS), 1602 (C=N), 766 (C–S). NMR data in DMSO-d_6: $\delta(^1H)$ 0.15 [s, 6H, $^2J(^{119/117}Sn–H)$ = 59.9 Hz, Sn–Me], 1.15 [s, 6H, ^2J(Pt–H) = 61.1 Hz, Pt–Me], 7.87 [br s, 2H, H^5], 8.35 [t, 2H, ^3J(HH) = 7.7 Hz, H^4], 8.83 [br s, 4H, $H^3$and H^6]; $\delta(^{13}C)$ −11.7 [s, ^1J(Pt–C) = 586 Hz, Pt–Me], −0.4 [s, $^1J(^{119/117}Sn–C)$ = 434, ^2J(Pt–C) = 84 Hz, Sn–Me], 124.3 (C^3), 127.0 (C^5), 140.0 (C^4), 148.1 (C^6), 155.0 (C^2); $\delta(^{119}Sn)$ −157 [s, ^1J(Pt–Sn) = not resolved]; $\delta(^{195}Pt)$ −3085 [s, ^1J(Pt-$^{119/117}$Sn) = 13192 Hz]. Single crystals of [$PtMe_2(SCN)_2(bpy)$] (**22**) suitable for X-ray crystallography study were obtained when the complex **17** was remained in chloroform at room temperature.

2.10. Preparation of [$PtMe_2(SnMe_2NCS)(SCN)(phen)$] (**18**)

Complex **18** was prepared in a similar way as for **17** except that [$PtMe_2(phen)$] was used instead of [$PtMe_2(bpy)$]. Yield: 53.8%; m.p. 213 °C (dec). Anal. Calc. for $C_{18}H_{20}N_4S_2PtSn$: C, 32.25; H, 3.01; N, 8.36; S, 9.57. Found C, 32.18; H, 3.19; N, 8.25; S, 9.59%. Selected IR data (KBr, cm^{-1}): 3047–2811 (C–H), 2103 (SCN), 2062 (NCS), 1517 (C=N), 773 (C–S). NMR data in DMSO-d_6: $\delta(^1H)$ −0.06 [s, 6H, $^2J(^{119/117}Sn–H)$ = 60.6 Hz, Sn–Me], 1.30 [s, 6H, ^2J(Pt–H) = 62.1 Hz, Pt–Me], 8.22 [dd, 2H, ^3J(HH) = 8.0 Hz, ^3J(HH) = 5.1 Hz, H^3], 8.34 [s, 2H, H^5], 8.97 [d, 2H, ^3J(HH) = 7.8 Hz, $H^{4,7}$], 9.19 [d, 2H, ^3J(HH) = 5.1 Hz, H^2]; $\delta(^{13}C)$ −12.2 [s, ^1J(Pt–C) = 592 Hz, Pt–Me], −0.6 [s, $^1J(^{119/117}Sn–C)$ = 454 Hz, ^2J(Pt–C) = 84 Hz, Sn–Me], 125.7 (C^3), 127.9 (C^5), 130.8 (C^{13}), 139.1 (C^4), 145.9 (C^{11}), 148.8 (C^2). $\delta(^{119}Sn)$ −372; $\delta(^{195}Pt)$ −3100 [s, ^1J(Pt-$^{119/117}$Sn) = 12656 Hz].

2.11. Preparation of [$PtMe_2(SnMe_2NCS)(SCN)(5,5'\text{-}Me_2bpy)$] (**19**)

This was prepared in a similar way as for **17** except that [$PtMe_2(5,5'\text{-}Me_2bpy$)] was used. Yield: 59%; m.p. 176–178 °C. Anal. Calc. for $C_{18}H_{24}N_4S_2PtSn$.acetone: C, 34.44; H, 4.13; N, 7.65; S, 8.75. Found: C, 34.88; H, 3.94; N, 7.28; S, 8.71%. Selected IR data (KBr, cm^{-1}): 3047–2817 (C–H), 2094 (SCN), 2054 (NCS), 1601 (C=N), 768 (C–S). NMR data in DMSO-d_6: $\delta(^1H)$ 0.11 [s, 6H, ^2J(Sn–H) = 60.9 Hz, Sn–Me], 1.15 [s, 6H, ^2J(Pt–H) = 60.9 Hz, Pt–Me], 2.53 [s, 6H, CH_3 of 5,5′-Me_2bpy], 8.15 [d, 2H, ^3J(HH) = 8.1 Hz, H^3], 8.59 [s, 2H, H^6], 8.65 [d, 2H, ^3J(HH) = 8.1 Hz, H^4]; $\delta(^{13}C)$ −11.6 [s, ^1J(Pt–C) = 587 Hz, Pt–Me], −0.7 [s, ^1J(Sn–C) = 415 Hz, ^2J(Pt–C) = 89 Hz, Sn–Me], 18.2 [s, CH_3 of 5,5′-Me_2bpy], 123.4 (C^4), 136.9 (C^5), 140.3 (C^3), 147.8 (C^6), 152.6 (C^2); $\delta(^{119}Sn)$ −153; $\delta(^{195}Pt)$ −3080. Single crystals of [$PtMe_2(SCN)_2(5,5'\text{-}Me_2bpy$)]. H_2O (**23**) suitable for X-ray crystallography study were obtained when the complex **19** was remained in DMSO solution at room temperature.

2.12. Preparation of [$PtMe_2(SnMe_2NCS)(SCN)(bu_2bpy)$] (**20**)

This was prepared in a similar way as for **17** except that [$PtMe_2(bu_2bpy$)] was used. Yield: 55%; m.p. 203 °C (dec). Anal. Calc.

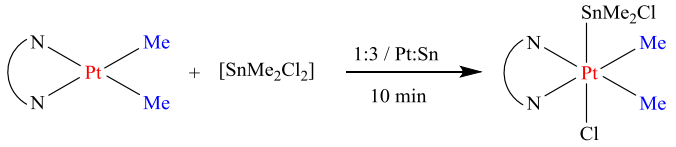

NN		NN	
4,4'-Me_2bpy	(3)	4,4'-Me_2bpy	(7)
5,5'-Me_2bpy	(4)	5,5'-Me_2bpy	(8)
bphen	(6)	bphen	(9)

Scheme 1. Preparation of organoplatinum(IV) complexes **7-9**.

for $C_{24}H_{36}N_4S_2PtSn$: C, 38.00; H, 4.78; N, 7.39; S, 8.45. Found: C, 38.56; H, 5.26; N, 6.48; S, 8.50%. Selected IR data (KBr, cm^{-1}): 2962–2904 (C–H), 2090 (SCN), 2055 (NCS), 1613 (C=N), 773 (C–S). NMR data in DMSO-d_6: $\delta(^1H)$ 0.13 [s, 6H, $^2J(^{119/117}Sn–H) = 61.6$ Hz, Sn–Me], 1.11 [s, 6H, $^2J(Pt–H) = 60.9$ Hz, Pt–Me], 1.44 [s, 18H, CH_3 of bu_2bpy], 7.82 [dd, 2H, $^3J(HH) = 6.0$ Hz, $^4J(HH) = 1.5$ Hz, H^5], 8.67 [d, 2H, $^4J(HH) = 1.5$ Hz, H^3], 8.75 [d, 2H, $^3J(HH) = 5.9$ Hz, H^6]; $\delta(^{13}C)$ −11.8 [s, $^1J(Pt–C) = 585$ Hz, Pt–Me], −0.4 [s, $^1J(^{119/117}Sn–C)$ = not resolved, $^2J(Pt–C) = 85$ Hz, Sn–Me], 30.3 (s, terminal C of ^tBu), 35.7 (s, central C of ^tBu), 121.2 (C^3), 123.6 (C^5), 149.2 (C^6), 155.4 (C^4), 163.8 (C^2). $\delta(^{119}Sn)$ −372; $\delta(^{195}Pt)$ −2755.

2.13. Preparation of [$PtMe_2$($SnMe_2NCS$)(SCN)(bphen)] (**21**)

This was prepared similarly but using [$PtMe_2$(bphen)] and the precipitate was washed with diethyl ether/pentane (1:1) and air dried. Yield: 24%; m.p. 188–190 °C. Anal. Calc. for $C_{30}H_{28}N_4S_2PtSn.2H_2O$: C, 41.97; H, 3.76; N, 6.53; S, 7.47. Found: C, 41.14; H, 3.56; N, 6.40; S, 7.47%. Selected IR data (KBr, cm^{-1}): 3044–2790 (C–H), 2111 (SCN), 2078 (NCS), 1598 (C=N), 719 (C–S). NMR data in $CDCl_3$: $\delta(^1H)$ 0.30 [s, 6H, $^2J(Sn–H) = 49.4$ Hz, Sn–Me], 1.38 [s, 6H, $^2J(Pt–H) = 57.7$ Hz, Pt–Me], 7.59–7.64 [m, 10H, Ph groups], 8.00 [d, 2H, $^3J(HH) = 5.4$ Hz, H^3], 8.12 [s, 2H, H^5], 9.17 [d, 2H, $^3J(HH) = 5.4$ Hz, $^3J(Pt–H) = 20.5$ Hz, H^2]; $\delta(^{13}C)$ −13.5 [s, $^1J(Pt–C) = 559$ Hz, Pt–Me], −5.1 [s, $^1J(Sn–C) = 305$ Hz, $^2J(Pt–C) = 84$ Hz, Sn–Me], 126.0–126.5 [m, C^5, C^6, C^3, C^8, C^{13}, C^{14}], 129.3–130.0 (m, Ph groups), 135.8 (C^1), 147.1 (C^2), 147.2 (C^{11}), 152.0 (C^4); $\delta(^{119}Sn)$ −11 [s, $^1J(Pt–Sn) = 11881$ Hz]; $\delta(^{195}Pt)$ −2798.

2.14. X-ray crystal structure determination

Single crystal X-ray diffraction experiments of **10**, **13**, **14**, **15**, **22** and **23** were performed on a KUMA KM-4 diffractometer with a two-dimensional area CCD detector. Yellow crystals (needle) were chosen, radiation Mo-Kα, λ = 0.71073 Å. Data collection was performed at low temperature (100(1) K) using the CrysAlis CCD program [44]. The ω-scan technique with Δω = 1.0° for each image was used for data collection. One image was used as a standard after every 40 images for monitoring of the crystal stability and data collection, and no correction on the relative intensity variations was necessary. Integration, scaling of the reflections, correction for Lorenz and polarization effects and absorption corrections were performed using the CrysAlis Red program [44]. The structures were solved by the direct methods using SHELXT program and refined on F^2 with a Full-matrix least-squares algorithm using the SHELXL (Sheldrick 2014/7) software [45]. A summary of crystal data, experimental details, and refinement results is given in Supplementary Information (Table S1).

3. Results and discussion

3.1. Preparation and characterization

As part of a study on the oxidative addition reactions of the electron rich organoplatinum(II) complexes [$PtMe_2$(NN)] {NN = bpy (**1**), phen (**2**), 4,4′-Me_2bpy (**3**), 5,5′-Me_2bpy (**4**), bu_2bpy (**5**) with diorganotin dichloride and diisothiocyanate, six diimine ligands were employed in this paper. Herein, we report the preparation of [$PtMe_2$(bphen)] (**6**) for the first time. The reaction of [$Pt_2Me_4(\mu\text{-}SMe_2)_2$] with bphen in acetone affords the red complex [$PtMe_2$(bphen) (**6**) in high yield. The complex **6** was characterized by elemental analysis, ^1H, ^{13}C, and ^{195}Pt NMR spectroscopy. The ^1H NMR spectrum of complex [$PtMe_2$(bphen)] (**6**) gives a resonance at $\delta = 1.30$ ppm with platinum satellites $^2J(Pt–H) = 85.3$ Hz due to the Pt–Me groups. In addition, the ^{13}C NMR spectrum of **6** in $CDCl_3$ displays a singlet of $\delta = -17.1$ ppm with $^1J(Pt–C) = 804$ Hz. The UV–visible spectrum of a solution of **6** in toluene shows two bands at 474 and 516 nm which arises from the Pt(5d) to π*(diimine) MLCT transitions [46].

Reaction of [$PtMe_2$(NN)] with $SnMe_2Cl_2$ in a 1:3/Pt:Sn mole ratio resulted in formation of new platinum(IV) complexes [$PtMe_2$($SnMe_2$Cl)Cl(NN)] {NN = 4,4′-Me_2bpy (**7**); 5,5′-Me_2bpy (**8**); bphen (**9**) in good yields (Scheme 1). The reactions occurred easily at room temperature and the reactions proceeded based on the color change from orange-red to pale yellow. Our data show that the oxidative addition reaction depends upon the Pt:Sn mole ratios as well as the reaction time.

The characterization of the products was established by elemental analysis, multinuclear (^1H, ^{13}C, ^{119}Sn, ^{195}Pt) NMR, and 2D NMR (HHCOSY, HSQC, and DEPT-135°) spectroscopy. The

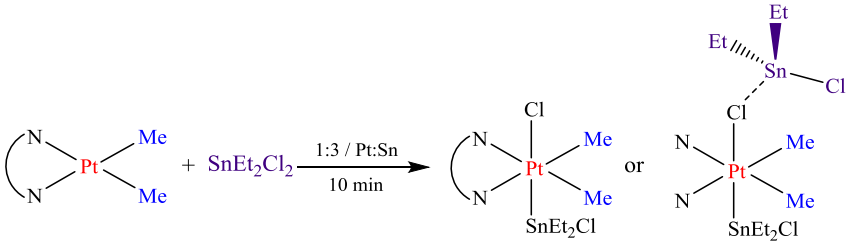

NN		NN		NN	
4,4'-Me_2bpy	(3)	4,4'-Me_2bpy	(11)	5,5'-Me_2bpy	(12)
5,5'-Me_2bpy	(4)			bu_2bpy	(13)
bu_2bpy	(5)				

Scheme 2. Preparation of complexes **11-13**.

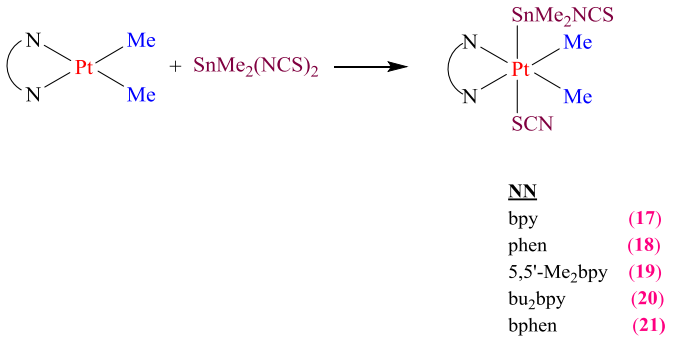

Scheme 3. Synthesis of complexes **17-21**.

observation of one Pt–Me resonance and a diimine ligand in complexes **7**–**9** indicate the *trans* oxidative addition occurred. The ^{1}H NMR spectra of platinum(IV) complexes **7**–**9** show a sharp resonance at $\delta = 1.33–1.55$ ppm with well resolved $^{2}J(Pt–H) = 55.7$ Hz and $\delta = 0.35–0.41$ ppm with $^{3}J(Sn–H) = 47.9–48.9$ Hz, the ^{1}H NMR spectra of complexes **7**–**9** are shown in Fig. S1. As an example, the ^{13}C NMR spectrum of complex [$PtMe_2(SnMe_2Cl)Cl$(bphen)] (**9**) in $CDCl_3$ contains a singlet at $\delta = -12.4$ ppm with $^{1}J(PtC) = 570$ Hz which is assigned to the Pt–CH_3 ligands. The signal due to the Sn–Me appears at $\delta = -3.4$ which is accompanied by tin and platinum satellites with $^{1}J(^{119/117}Sn–C) = 300$ Hz and $^{2}J(Pt–C) = 100$ Hz (Fig. S2). The DEPT-135° spectrum of complex **9** confirms the structural information by elimination of the signals of quaternary carbons (Fig. S3). The assignments of the diimine ligand are made by a correlation in the HSQC spectrum (Fig. S4).

The presence of tin satellites $^{1}J(Pt-^{119/117}Sn) = 12360–13082$ Hz in the ^{195}Pt NMR spectra as well as the platinum satellites $^{1}J(Pt–Sn) = 12878–12964$ Hz in the ^{119}Sn NMR spectra of complexes **7**–**9** indicate that the direct platinum-tin bond is maintained in solution, the ^{195}Pt and ^{119}Sn NMR spectra of complexes **7**–**9** are shown in Fig. S5. It should be mentioned that the free $SnMe_2Cl_2$ could not be detected in the case of **7**–**9** based on the elemental analysis and NMR spectra.

Similarly, the reactions of **3**–**5** with $SnEt_2Cl_2$ occurred to give the corresponding products of *trans* oxidative addition of organoplatinum(IV) complexes [$PtMe_2(SnEt_2Cl)Cl$(4,4′-Me_2bpy)] (**11**), [$PtMe_2(SnEt_2Cl)Cl$(5,5′-Me_2bpy)].$SnEt_2Cl_2$ (**12**) and [$PtMe_2(SnEt_2Cl)Cl$(bu_2bpy)].$SnEt_2Cl_2$ (**13**) since the resulting platinum(IV) complexes only one Pt–Me resonance as well as the signals for the magnetically equivalent diimine ligands (Scheme 2).

As an example, the ^{1}H NMR spectrum of [$PtMe_2(SnEt_2Cl)Cl$(4,4′-Me_2bpy)] (**11**) in $CDCl_3$ is shown in Fig. S6. In solution, these complexes are not stable for several days and the dissociation of stannyl group could be observed. Therefore, the diethylstannyl complexes **11**–**13** have the lower stability than the dimethylstannyl complexes **7**–**9** and dissociate in solution faster than the dimethyl analogues as indicated by NMR spectra. The observation of ^{195}Pt and ^{119}Sn satellites are direct proofs for the presence of covalent platinum-tin bonds in solution; the ^{195}Pt and ^{119}Sn NMR spectra of **11** and **12** are shown in Fig. S7. Notably, the complexes **12**–**13** form a 1:1 adduct with $SnEt_2Cl_2$, however, the adduct formation in the case of $SnMe_2Cl_2$ has been observed only in the case of crystallization in the presence of excess $SnMe_2Cl_2$ [13]. This can be attributed to the higher ability of $SnEt_2Cl_2$ towards adduct formation with Pt–Cl bond of organoplatinum(IV) compounds.

The platinum(II) complex PtClMe(4,4′-Me_2bpy)] (**14**) was obtained during the crystallization of a mixture of [$PtMe_2$(4,4′-Me_2bpy)] and excess of $SnEt_2Cl_2$. On the other hand, the ladder tetramer complex of [$Sn_4Et_8Cl_2O_2(OH)_2$] (**15**) was also obtained in an attempt to recrystallize [$PtMe_2(SnEt_2Cl)Cl$(5,5′-Me_2bpy)].$SnEt_2Cl_2$ in DMSO which is probably due to the partial hydrolysis of $SnEt_2Cl_2$ in solution. Moreover, the platinum(II) complex of [$PtCl_2$(bu_2bpy)] (**16**) was characterized by X-ray crystallography from the crystallization of [$PtMe_2(SnEt_2Cl)Cl$(bu_2bpy)].$SnEt_2Cl_2$ in a mixture of CH_2Cl_2 and n-pentane. The X-ray crystallography data reveals the formation of the yellow form of [$PtCl_2$(bu_2bpy)]; the crystal structure of **16** has already been published [47].

The oxidative addition of $SnMe_2(SCN)_2$ to [$PtMe_2$(NN)] proceeds rapidly and cleanly to give the corresponding platinum(IV) products [$PtMe_2(SnMe_2NCS)(SCN)$(NN)] {NN = bpy (**17**); phen (**18**); 5,5′-Me_2bpy (**19**); bu_2bpy (**20**), bphen (**21**)} in good yields. (Scheme 3). This is the first example of Sn–SCN cleavage in reactions with organoplatinum(II) complexes. As an example, the changes in the MLCT bands due to the reaction of [$PtMe_2$(4,4′-Me_2bpy)] with $SnMe_2(SCN)_2$ was followed by monitoring the decay of the MLCT bands as the reaction progressed (Fig. 1).

Compound **17**–**20** are almost insoluble in all common organic solvents except DMSO. For example, the ^{1}H and ^{13}C NMR spectra of complexes **17** and **19** in DMSO-d_6 demonstrate the *trans* oxidative addition of $SnMe_2(SCN)_2$ (Figs. S8–S9).

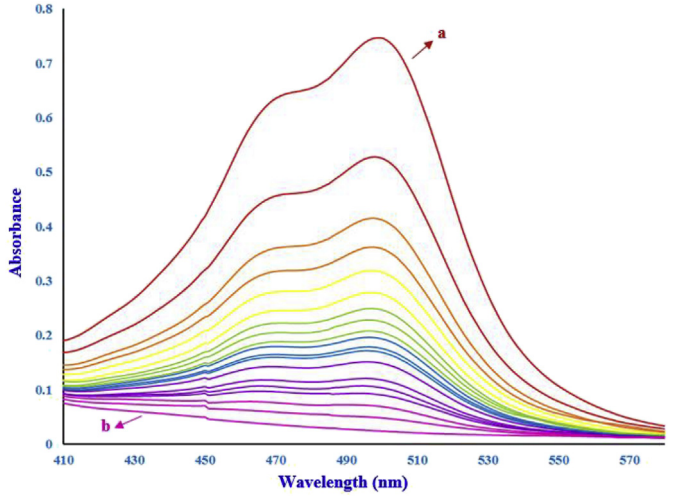

Fig. 1. Changes in the UV–Vis spectrum during the reaction of 3 mL [$PtMe_2$(4,4′-Me_2bpy)] (**3**) (3×10^{-4} M) with $SnMe_2(SCN)_2$ in a 1:1 mol ratio in toluene at room temperature, (a) pure [$PtMe_2$(4,4′-Me_2bpy)] (**3**) (b) after 1½ h; successive spectra recorded at intervals of 90 s.

Table 1
^{119}Sn and ^{195}Pt NMR data for platinum complexes.

Complexes	^{119}Sn		^{195}Pt	
	δ(ppm)	^{1}J(Pt–Sn) (Hz)	δ(ppm)	$^{1}J(Pt-^{119/117}Sn)$ (Hz)
6[a]	–	–	−3359	–
7[a]	17	12964	−2884	13082 and 12422
8[a]	19	12900	−2886	12963 and 12360
9[a]	19	12878	−2918	12947
11[a]	25	11595	−2838	11590 and 11090
12[a]	28	11446	−2833	11590 and 11132
13[a]	25	11526	−2838	11686
17[b]	−157	c	−3085	13192
18[b]	−372[d]	c	−3100	12656
19[b]	−153	c	−3080	c
20[b]	−372[d]	c	−2755	c
21[a]	−11	11881	−2798	c

[a] In $CDCl_3$; [b]in DMSO-d_6; [c] not resolved; [d] this is mainly due to the adduct formation of [$SnMe_2(NCS)_2(DMSO)_2$] upon remaining in solution.

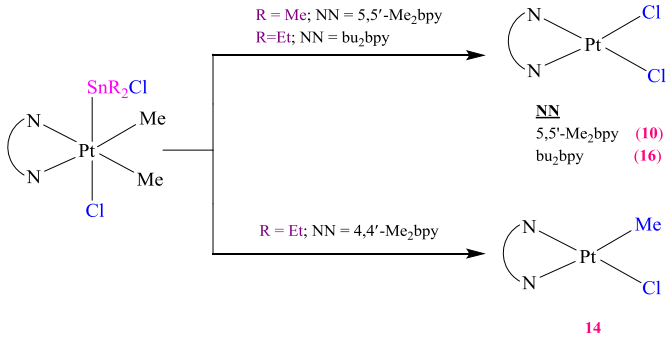

Scheme 4. Formation of platinum(II) complexes.

Note that the reactions of [$PtMe_2$(bu_2bpy)] and [$PtMe_2$(phen)] with $SnMe_2(SCN)_2$ resulted in formation of the yellow products which have been characterized as [$PtMe_2$($SnMe_2NCS$)(SCN)(NN)] {NN = phen (**18**), bu_2bpy(**20**)} using elemental analysis. However, there was a major product in NMR spectra, identified as [$SnMe_2(NCS)_2(DMSO)_2$]. NMR data displayed the complexes **18** and **20** existed in solution mainly in dissociated form due to the reversible oxidative addition of [$SnMe_2(NCS)_2$] to [$PtMe_2$(NN)] in DMSO-d_s. The ^{119}Sn NMR of a solution of [$SnMe_2(NCS)_2$] in DMSO-d_6 indicates a signal at $\delta = -379$ ppm. Therefore, the ^{119}Sn NMR spectra of **18** and **20** mostly reveals the adduct formation of [$SnMe_2(NCS)_2(DMSO)_2$] in solution.

Table 1 summarizes the ^{195}Pt and ^{119}Sn NMR data for the prepared complexes in this paper. It can be seen that the magnitude of the platinum-tin coupling constants of diethylstannylplatinum complexes are at the low end of the range found herein, indicating the weaker Pt–Sn interaction.

3.2. Reductive elimination or α-elimination of $SnMe_2$

It has been reported that organotin(IV) chlorides can undergo reversible oxidative addition to dimethylplatinum(II) compounds which can be followed by elimination of $SnMe_3Cl$, $SnMe_4$ and $SnMe_2$ [33,38]. The mechanism of electrophilic Pt–Me bond cleavage plays an important role in organometallic chemistry due to the selectivity of the site attack [2]. The formation of [PtMeCl(4,4′-Me_2bpy)] (**14**) involves the elimination of $SnMe_2EtCl$ from Pt(IV) complex (Scheme 4).

The reductive elimination of $SnEt_2MeCl$ is expected for the formation of platinum(II) complex [PtMeCl(4,4′-Me_2bpy)] (**14**) which should be intramolecular, as compared by analogy with similar reductive eliminations [38] (Scheme 5). Moreover, the elimination of $SnMe_3Cl$ and $SnEt_2MeCl$ are suggested for the formation of dichloroplatinum(II) complexes **10** and **16**.

The suitable single crystals of [$PtMe_2(SCN)_2$(bpy)] (**22**) were formed from a solution of **17** in chloroform while the single crystals of [$PtMe_2(SCN)_2$(5,5′-Me_2bpy)] (**23**) were grown from a saturated

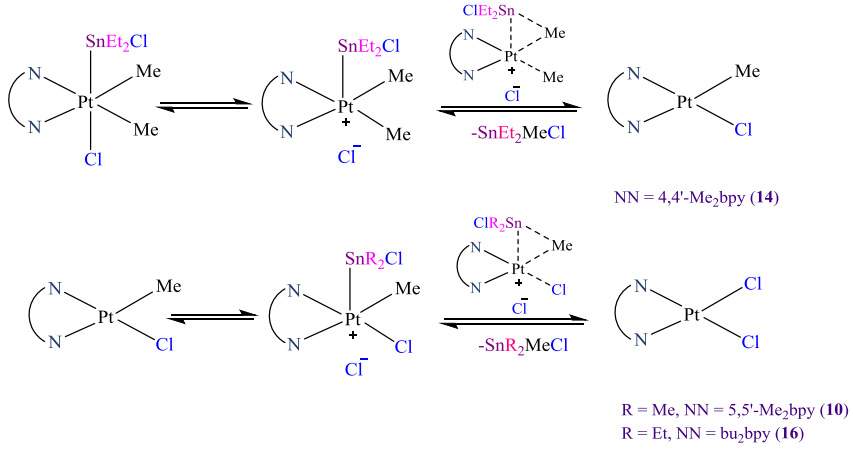

Scheme 5. Proposed mechanisms for the formation of platinum(II) complexes **10**, **14** and **16**.

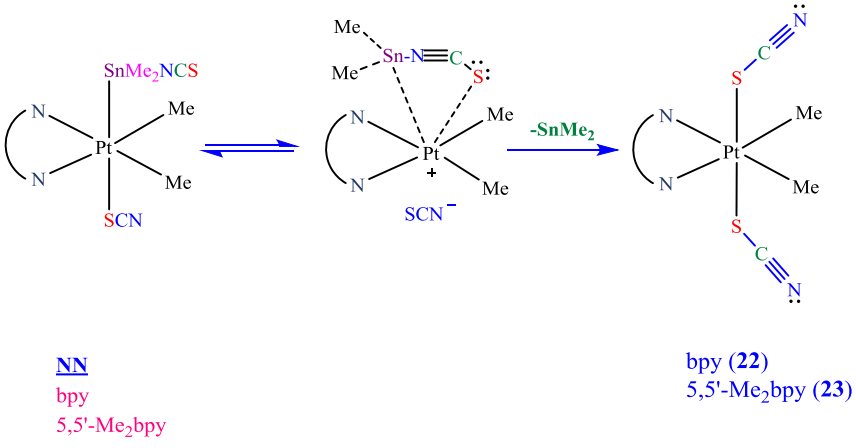

Scheme 6. Suggested mechanism for the formation of bis(thiocyanato)organoplatinum(IV) complexes **22-23**.

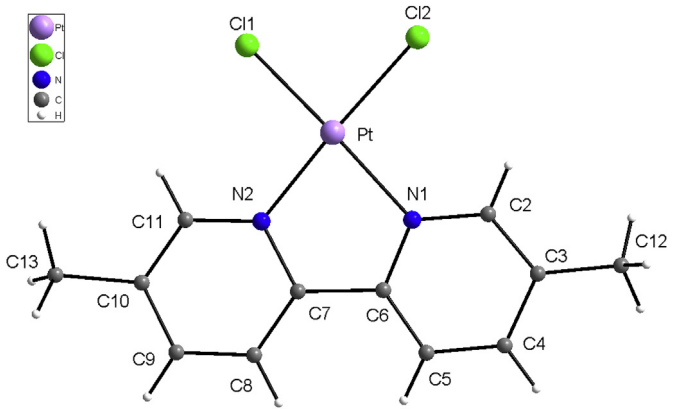

Fig. 2. ORTEP diagram of [$PtCl_2$(5,5′-Me_2bpy)] (**10**). Selected bond distances (Å) and angles (°): Pt–N2 2.026(5), Pt–N1 2.085(5), Pt–Cl1 2.164(4), Pt–Cl2 2.255(2), N2–Pt–N1 80.5(2), N2–Pt–Cl1 97.53(19), N1–Pt–Cl1 177.79(18), N2–Pt–Cl2 175.39(16), N1–Pt–Cl2 96.30(17), Cl1–Pt–Cl2 85.68(13).

solution of **19** in DMSO. It can be seen that in the case of X = SCN, α-elimination of $SnMe_2$ occurs to give [$PtMe_2$(SCN)$_2$(bpy)]. Elimination of $SnMe_2$ has already been observed in the case of [$PtMe_2$($SnMe_3$)Cl(bpy)] [38]. Therefore, the possible mechanism for elimination of $SnMe_2$ in **22**–**23** involves the transfer of NCS to platinum *via* the formation of linkage isomerism of Sn–N≡C–S–Pt, followed by Pt–Sn cleavage (Scheme 6). This mechanism supports the formation of Pt–SCN (thiocyanato) group.

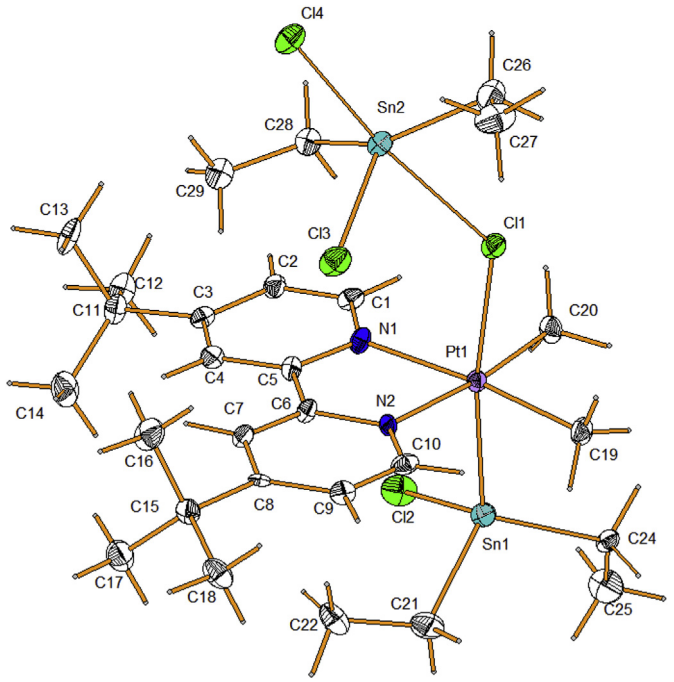

Fig. 3. ORTEP diagram of [$PtMe_2$($SnEt_2$Cl)Cl(bu_2bpy)].$SnEt_2Cl_2$ (**13**). Selected bond distances (Å) and angles (°): Pt1–C20 2.055(5), Pt1–C19 2.069(5), Pt1–N2 2.122(4), Pt1–N1 2.125(4), Pt1–Sn1 2.5399(4), Pt1–Cl1 2.5871(13), Sn1–C21 2.147(5), Sn1–C24 2.169(5), Sn1–Cl2 2.3951(14), Sn2–C26 2.138(6), Sn2–C28 2.138(5), Sn2–Cl3 2.3699(14), Sn2–Cl4 2.4890(13), Sn2–Cl1 2.8096(13), C20–Pt1–C19 90.2(2), C20–Pt1–N2 173.19(17), C19–Pt1–N2 96.48(19), N2–Pt1–N1 77.59(16), C20–Pt1–Sn1 86.11(15), C19–Pt1–Sn1 82.48(16), N2–Pt1–Sn1 95.93(11), N1–Pt1–Sn1 95.07(11), C20–Pt1–Cl1 89.36(16), C19–Pt1–Cl1 90.37(16), N2–Pt1–Cl1 89.39(12), N1–Pt1–Cl1 92.52(12), Sn1–Pt1–Cl1 171.51(3), C21–Sn1–Pt1 118.07(16), C24–Sn1–Pt1 113.37(14), Cl2–Sn1–Pt1 105.98(4), Pt1–Cl1–Sn2 133.36(5), C26–Sn2–C28 143.9(2), C26–Sn2–Cl3 107.74(17), C28–Sn2–Cl3 107.00(15), C26–Sn2–Cl4 92.22(16), C28–Sn2–Cl4 93.40(14), Cl3–Sn2–Cl4 96.33(5), C26–Sn2–Cl1 83.96(16), C28–Sn2–Cl1 86.47(14), Cl3–Sn2–Cl1 90.20(4), Cl4–Sn2–Cl1 173.21(5), Cl3–Sn2–Cl4 96.33(5).

3.3. Description and discussion of the crystal structures

An ORTEP drawing for [$PtCl_2$(5,5′-Me_2bpy)] (**10**) is shown in Fig. 2. The crystal structure of **10** shows that Pt(II) center adopts an almost square-planar geometry as the *trans* bond angles of Cl1–Pt–N1 and Cl2–Pt–N2 reveal little deviation from planarity (177.79(18) and 175.39(16) °, respectively). Two inequivalent Pt–Cl bond distances (2.164(4) and 2.255(2) Å) are noted which are shorter than those of yellow form of [$PtCl_2$(bpy)] (2.281(4) and 2.300(3) Å) [48] and red form of [$PtCl_2$(bpy)] (2.306(2) Å) [49], yellow form of [$PtCl_2$(bu_2bpy)] (2.293(3) and 2.287(4) Å) [47], [$PtCl_2$(phen)] (2.311(3) and 2.305(3) Å) [50], [$PtCl_2$(4,4′-Me_2bpy)] (2.304(1) and 2.292(1) Å) [51], and [$PtCl_2$(6,6′-Me_2bpy)] (2.3034(9) and 2.3015(7) Å) [51] due to the lower *trans* influence of 5,5′-Me_2bpy. The flat molecules stack in *c* direction in a head to tail fashion with Pt···Pt distances of 7.3930(4) Å. The 5,5′-Me_2bpy groups are anti to each other. The Pt···Pt separation is too long to support a metal … metal interaction while the separation between 5,5′-Me_2bpy is 3.690 Å which confirms the presence of the yellow form of [$PtCl_2$(5,5′-Me_2bpy)] in the solid state (Fig. S10).

The structure of complex [$PtMe_2$($SnEt_2$Cl)Cl(bu_2bpy)].$SnEt_2$Cl (**13**) is shown in Fig. 3. The structure confirms the coordination of chloride from Pt–Cl bond to the $SnEt_2Cl_2$. The equatorial angles at the Sn2 center are significantly distorted from ideal 120° as revealed by the C28–Sn2–Cl3 (107.00(15)°), Cl3–Sn2–C26 (107.74(17)°) and C28–Sn2–C26 (143.9(2)°). Approximately distorted trigonal bipyramidal geometry about the Sn2 center of free $SnEt_2Cl_2$ results from the coordination of the chloride from Pt–Cl bond to tin, affording Cl···$SnEt_2Cl_2$ (Cl1···Sn2–Cl4 angle of 173.21(5)°). The Sn–Cl bond distances follow bridging Sn2–Cl1 (2.8096(13) Å) ≫ axial Sn2–Cl4 (2.4890(13) Å) > equatorial Sn2–Cl3 (2.3699(14) Å). The Pt–Cl bond distance is 2.5871(13) Å which is considerably longer than that of observed for [$PtMe_2$(Sn-Me_2Cl)Cl(bu_2bpy)].$SnMe_2Cl_2$ (2.480(2) Å) [13] which reveals the higher *trans* influence of $SnEt_2$Cl relative to $SnMe_2$Cl. The crystal

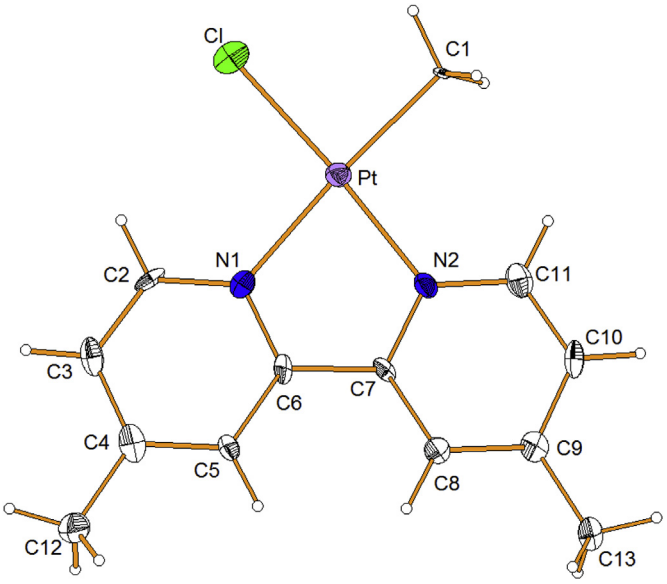

Fig. 4. View of the molecular structure of [PtMeCl(4,4′-Me_2bpy)] (**14**). Selected bond distances (Å) and angles (°): Pt–N2 2.032(6), Pt–C1 2.088(6), Pt–N1 2.092(6), Pt–Cl 2.284(2), N2–Pt–C1 95.9(2), N2–Pt–N1 79.6(2), C1–Pt–N1 175.0(2), N2–Pt–Cl 175.91(16), C1–Pt–Cl 88.14(18), N1–Pt–Cl 96.29(16).

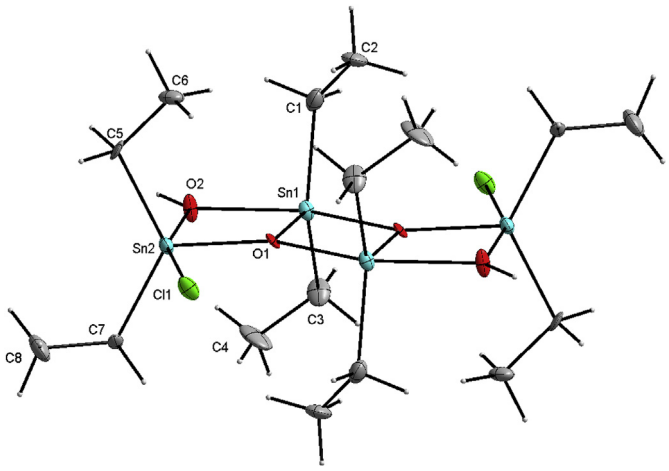

Fig. 5. ORTEP diagram of $[Sn_4(C_2H_5)_8Cl_2O_2(OH)_2]$ (**15**). Selected bond distances (Å) and angles (°): Sn1–O1 2.063(5), Sn1–C3 2.118(9), Sn1–C1 2.115(9), Sn1–O1 2.142(5), Sn1–O2 2.190(6), O1–Sn2 2.013(6), O1–Sn1 2.142(5), O2–Sn2 2.147(5), Sn2–C7 2.115(9), Sn2–C5 2.131(8), Sn2–Cl1 2.565(2), O1–Sn1–C3 116.8(3), O1–Sn1–C1 114.6(3), C3–Sn1–C1 128.4(4), O1–Sn1–O1 73.5(2), C3–Sn1–O1 98.6(3), C1–Sn1–O1 100.3(3), O1–Sn1–O2 72.2(2), C3–Sn1–O2 97.2(3), C1–Sn1–O2 93.4(3), O1–Sn1–O2 145.69(19), Sn2–O2–Sn1 102.0(2 74.1(2), C7–Sn2–O2 98.7(3), C5–Sn2–O2 95.6(3), O1–Sn2–Cl1 84.34(16), C5–Sn2–Cl1 92.8(2), O2–Sn2–Cl1 158.45(17).

packing of **13** indicates the presence of the several hydrogen bonding contacts which plays an important role in the stabilization of the crystal packing (Fig. S11).

An ORTEP of [PtMeCl(4,4′-Me_2bpy)] (**14**) is presented in Fig. 4. The expected square-planar coordination geometry is observed at platinum atom that is defined by two nitrogen atoms from the 4,4′-Me_2bpy ligand and one chlorine atom and a methyl group. As expected, the Pt–N1 bond distance, *trans* to σ-carbon, is longer that of Pt–N2 due to the higher *trans* influence of the Me. The centroid···centroid distance of Cg1-Cg2 is 3.697 Å (Cg1 and Cg2 are the centroids of the rings formed by N1–C7–C8–C9–C10–C11 and N1–C2–C3–C4–C5–C6) points out the presence of π-π interaction. The shortest Pt···Pt intermolecular distance is 6.3201(6) Å (Fig. S12).

The tetranuclear ladder-type structure of $[Sn_4(C_2H_5)_8Cl_2O_2(OH)_2]$ (**15**) is shown in Fig. 5. The crystal structure of **15** reveals that tin atoms Sn1 and Sn2 are incorporated in two symmetry related four-membered rings Sn2O2. Each ladder consists of two tin centers, two $SnEt_2$ and $SnEt_2Cl$ unites are bridged by the hydroxo and oxo groups. Both exocyclic tin atoms Sn2 and endocyclic Sn1 are five-coordinate that adopts a distorted trigonal bipyramidal geometry as distorted by linearity (O1–Sn1–O2 = 145.69(19) and O2–Sn2–Cl1 = 158.45(17)). The ethyl groups are located in the equatorial positions and the Cl bonded to Sn(2) (2.565(2) Å) occupies an axial site. Two intermolecular hydrogen bonds of O2–H2···Cl1 (3.207(6) Å) and C7–H7A … Cl1 (3.614(9) Å) are present in the crystal packing (Fig. S13).

The crystal structure of complexes $[PtMe_2(SCN)_2(bpy)]$ (**22**) and $[PtMe_2(SCN)_2(5,5'\text{-}Me_2bpy)]$. H_2O (**23**) are of particular interest and structurally unique in this study as shown in Fig. 6 and Fig S14, respectively. The crystal structures of **22** and **23** shows that each of platinum has a slightly distorted octahedral geometry. In both complexes **22** and **23**, pairs of thiocyanate ligands are disposed *trans* to each other. There are two independent molecules in each unit cell which differ mainly by the Pt–SCN angles. The coordination geometries of the complexes **22**–**23** are similar and SCN groups are bonded to platinum through the sulfur atom, Pt–SCN (thiocyanate). The Pt–S–C bond angles are expected to be bent according to the VSEPR-predicted bond angle ≤109.5° which confirms with the values of 101–104° for **22** and **23**. The crystal packing of **22** reveals the presence of intramolecular and intermolecular hydrogen bonds between C–H and SCN groups as shown in Fig. S15. On the other hand, the crystal packing of **23** reveals a hydrogen bonded dimer *via* a water molecule which has resulted in the formation of a supramolecular network. Moreover, there are several intramolecular and intermolecular hydrogen bonds between H_2O and SCN groups as well as hydrogen bonds between C–H and SCN groups (Fig. S16).

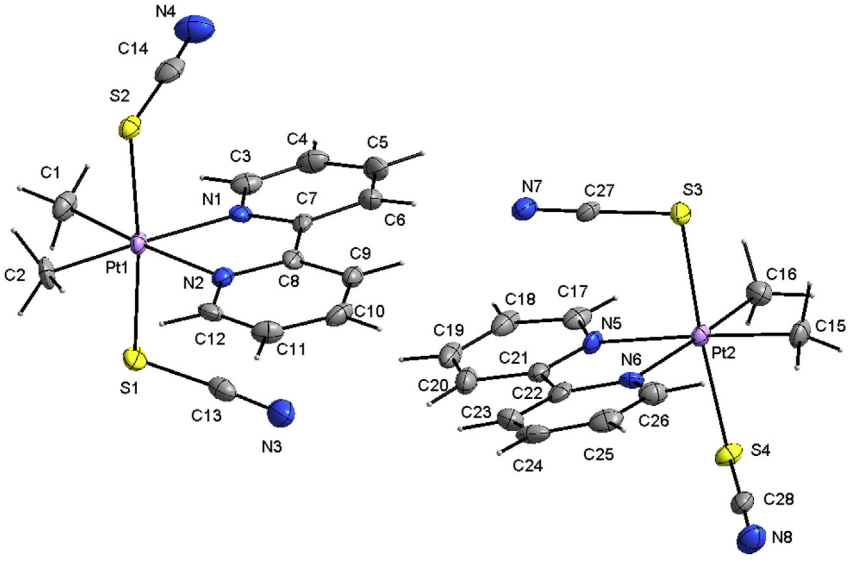

Fig. 6. ORTEP diagram of $[PtMe_2(SCN)_2(bpy)]$ (**22**). Selected bond distances (Å) and angles (°): Pt1–C2 2.052(5), Pt1–C1 2.070(5), Pt1–N1 2.149(4), Pt1–N2 2.176(4), Pt1–S2 2.3520(14), Pt1–S1 2.3549(14), Pt2–C15 2.064(5), Pt2–C16 2.069(6), Pt2–N6 2.146(4), Pt2–N5 2.161(4), Pt2–S3 2.3548(14), Pt2–S4 2.3582(14), C2–Pt1–C1 86.3(2), C2–Pt1–N1 174.78(18), C1–Pt1–N1 98.8(2), C2–Pt1–N2 97.95(18), C1–Pt1–N2 175.6(2), N1–Pt1–N2 76.89(15), C2–Pt1–S2 86.35(17), C1–Pt1–S2 89.77(16), N1–Pt1–S2 92.83(11), N2–Pt1–S2 89.63(11), C2–Pt1–S1 89.54(17), C1–Pt1–S1 86.49(16), N1–Pt1–S1 91.57(11), N2–Pt1–S1 94.39(11), S2–Pt1–S1 174.61(5), C8–N2–Pt1 114.3(3), C13–S1–Pt1 102.46(19), C14–S2–Pt1 102.1(2), C15–Pt2–C16 86.5(2), C15–Pt2–N6 98.6(2), C16–Pt2–N6 174.84(18), C15–Pt2–N5 175.1(2), C16–Pt2–N5 98.31(19), N6–Pt2–N5 76.54(16), C15–Pt2–S3 87.56(16), C16–Pt2–S3 89.01(16), N6–Pt2–S3 91.60(12), N5–Pt2–S3 93.05 (11), C15–Pt2–S4 90.29(16), C16–Pt2–S4 87.21(16), N6–Pt2–S4 92.33(12), N5–Pt2–S4 89.40(12), S3–Pt2–S4 175.76(5), C21–N5–Pt2 115.0(3), C17–N5–Pt2 124.4(4), C26–N6–Pt2 125.5(4), C22–N6–Pt2 116.2(3), C27–S3–Pt2 101.85(18), C28–S4–Pt2 101.7(2), N7–C27–S3 178.9(5), N8–C28–S4 176.8(5), N3–C13–S1 176.9(5), N4–C14–S2 177.1(6).

4. Conclusion

In conclusion, we have successfully synthesized and characterized a range of organoplatinum(II) complexes including a variety of rigid and bidentate diimine ligands containing diorganotin dihalides or pseudohalides to investigate the role of alkyl (Me or Et) and halides (Cl or SCN). The most remarkable feature of the oxidative addition with $SnEt_2Cl_2$ is the adduct formation with the second molecule of $SnEt_2Cl_2$ in two cases. These reactions are strongly dependent on the molar ratios, reaction time and solvent. This study suggests that the more complex reaction mechanisms are possible besides the competitive pathways of oxidative addition and reductive elimination. The oxidative addition reaction of Sn–SCN to the organoplatinum(II) was reported for the first time to afford the novel organoplatinum(IV) complexes [$PtMe_2$($SnMe_2$NCS)(SCN)(NN)]. Accordingly, a wide range of platinum complexes can be prepared *via* oxidative addition of Sn-pseudohalide that are stable enough to allow their structures to be studied in great detail. However, they dissociate in solution to give [$PtMe_2(SCN)_2$(NN)] *via* α-elimination of $SnMe_2$ to give new bis(pseudohalido)platinum(IV) complexes. The NMR monitoring data exhibited that diethylstannylplatinum(IV) complexes dissociate faster, as compared to dimethyl analogues. Qualitatively, the order of stability of the stannylorganoplatinum(IV) compounds varies according to the trends [$PtMe_2$($SnMe_2$Cl)Cl(NN)]> [$PtMe_2$($SnMe_2$NCS)(SCN)(NN)]>[$PtMe_2$($SnEt_2$Cl)Cl(NN)], as these compounds show a tendency to undergo reductive elimination or α-elimination. Moreover, X-ray crystallography data confirms the higher *trans* influence of $SnEt_2Cl$ relative to $SnMe_2Cl$. In general, platinum complexes [$PtCl_2$(NN)], [PtClMe(NN)] and [$PtMe_2(SCN)_2$(NN)] could be formed during the dissociation of the organoplatinum(IV) products due to the elimination of organotin compounds.

Acknowledgements

We would like to thank the Science Research Council of K.N. Toosi University of Technology for financial support. The authors would like to express their deepest gratitude to Professor Mehdi Rashidi, who passed away last year, for his outstanding contribution to the field of Organometallic Chemistry in Iran.

Appendix A. Supplementary data

Supplementary data to this article can be found online at https://doi.org/10.1016/j.jorganchem.2018.11.022.

References

[1] J.K. Stille, The palladium-catalyzed cross-coupling reactions of organotin reagents with organic electrophiles, Angew. Chem. Int. Ed. 25 (1986) 508–524.
[2] P. Espinet, A.M. Echavarren, The mechanisms of the stille reaction, Angew. Chem. Int. Ed. 43 (2004) 4704–4734.
[3] Q. Chen, Y. Yang, X. Lin, W. Ma, G. Chen, W. Li, X. Wang, Z. Yu, Platinum(IV) prodrugs with long lipid chains for drug delivery and overcoming cisplatin resistance, Chem. Commun. 54 (2018) 5369–5372.
[4] C.S.A. Fraser, H.A. Jenkins, M.C. Jennings, R.J. Puddephatt, Organoplatinum(IV) complexes with hydrogen bonds: from monomers to polymers, Organometallics 19 (2000) 1635–1642.
[5] L.M. Rendina, R.J. Puddephatt, Oxidative addition reactions of organoplatinum(II) complexes with nitrogen-donor ligands, Chem. Rev. 97 (1997) 1735–1754.
[6] M. Safa, R.J. Puddephatt, Chelating imidazole ligands promote oxidative addition in dimethylplatinum(II) complexes, J. Organomet. Chem. 761 (2014) 42–50.
[7] N.L.S. Yue, M.C. Jennings, R.J. Puddephatt, Dimerization of an organoplatinum complex triggered by oxidative addition: a model for dynamic ring-opening polymerization, J. Organomet. Chem. 803 (2016) 45–50.
[8] A. Abo-Amer, R.J. Puddephatt, Reactivity and mechanism in the ring-opening of cyclopropylmethylplatinum(IV) complexes, Inorg. Chem. Commun. 14 (2011) 111–114.
[9] A.J. Canty, A.A. Watson, Organopalladium(IV) chemistry: binuclear Pd^{IV}-Pd^{IV} and Pd^{IV}-Pt^{IV} μ-hydrocarbyl complexes, Inorg. Chim. Acta. 154 (1988) 5–7.
[10] R.H.W. Au, M.C. Jennings, R.J. Puddephatt, Binuclear platinum(IV) complexes with bridging amidoalkyl groups and their self-assembly through hydrogen bonding, Organometallics 28 (2009) 3734–3743.
[11] M.C. Janzen, M.C. Jennings, R.J. Puddephatt, Double oxidative addition of tin(IV) halides to platinum(II): complexes with Pt-Sn and Pt-Sn-Pt linkages, Organometallics 20 (2001) 4100–4106.
[12] M. Rashidi, B.Z. Momeni, ω-Monobromoalkyl platina(IV)cyclopentane complexes: synthesis, characterization and kinetic studies of the formation, J. Organomet. Chem. 574 (1999) 286–293.
[13] M.C. Janzen, M.C. Jennings, R.J. Puddephatt, Self-assembly using stannylplatinum(IV) halide complexes as ligands for organotin halides, Can. J. Chem. 80 (2002) 1451–1457.
[14] E.M. Prokopchuk, R.J. Puddephatt, Dimethylplatinum(IV) chemistry: stannyl, hydride, hydroxide, and aqua complexes, Can. J. Chem. 81 (2003) 476–483.
[15] B.Z. Momeni, N. Fathi, A. Mohagheghi, Easy oxidative addition of the carbon-halogen bond by dimethylplatinum(II) complexes containing a related series of diimine ligands: synthesis, spectral characterization and crystal structure, J. Mol. Struct. 1079 (2015) 281–290.
[16] T. Okujima, S. Ito, N. Morita, Preparation and Stille cross-coupling reaction of the first organotin reagents of azulenes. An efficient Pd(0)-catalyzed synthesis of 6-aryl- and biazulenes, Tetrahedron Lett. 43 (2002) 1261–1264.
[17] J.K. Stille, Palladium catalyzed coupling of organotin reagents with organic electrophiles, Pure Appl. Chem. 57 (1985) 1771–1780.
[18] I. Schwager, J.F. Knifton, Homogeneous olefin hydroformylation catalyzed by ligand stabilized platinum(ll)-group IVB metal halide complexes, J. Catal. 45 (1976) 256–267.
[19] A. Scrivanti, G. Cavinato, L. Toniolo, C. Botteghi, Metals in organic syntheses: XI. ^{31}P NMR and reactivity studies on the system *trans*-[PtCl(CO-n-hexyl)(PPh_3)$_2$]/$SnCl_2$, an active intermediate in the catalytic hydroformylation of 1-hexene, J. Organomet. Chem. 286 (1985) 115–120.
[20] A. Scrivanti, S. Paganelli, U. Matteoli, C. Botteghi, Further studies of the Pt^{II}/$SnCl_2$ catalyzed hydroformylation, J. Organomet. Chem. 385 (1990) 439–446.
[21] D. Fernández, M.I. García-Seijo, T. Kégl, G. Petőcz, L. Kollár, M.E. García-Fernández, Preparation and structural characterization of ionic five-coordinate palladium(II) and platinum(II) complexes of the ligand tris[2-(diphenylphosphino)ethyl]phosphine. Insertion of $SnCl_2$ into M-Cl bonds (M = Pd, Pt) and hydroformylation activity of the Pt-$SnCl_3$ systems, Inorg. Chem. 41 (2002) 4435–4443.
[22] H.C. Clark, J.A. Davies, The hydroformylation reaction: catalysis by platinum(II)-tin(II) systems, J. Organomet. Chem. 213 (1981) 503–512.
[23] R. Tarozaitė, L. Tamašauskaitė Tamašiūnaitė, V. Jasulaitienė, Platinum-tin complexes as catalysts for the anodic oxidation of borohydride, J. Solid State Electrochem. 13 (2009) 721–731.
[24] C.J. Levy, J.J. Vittal, R.J. Puddephatt, Synthesis and characterization of group 14-platinum(IV) complexes, Organometallics 15 (1996) 2108–2117.
[25] W.M. Teles, N.L. Speziali, C.A.L. Filgueiras, Synthesis of a polymetallic Pt, Sn complex containing square planar and trigonal bipyramidal platinum centres. Crystal and molecular structure of bis{chlorotriethylphosphinoplatinum(II)}μ-2,3,5,6-tetrakis(α-pyridyl)-pyrazinetetrakis(trichlorostannyl)triethylphosphinoplatinate(II), Polyhedron 19 (2000) 739–742.
[26] L. Kollár, S. Gladiali, M.J. Tenorio, W. Weissensteiner, Formation of platinum-tin bond by tin(II)chloride insertion, J. Cluster Sci. 9 (1998) 321–328.
[27] S.H.L. Thoonen, M. Lutz, A.L. Spek, B.-J. Deelman, G. van Koten, Synthesis of novel trialkyl(trichlorostannyl)platinum(IV) complexes through $SnCl_2$ insertion into the Pt-Cl bond, Organometallics 22 (2003) 1156–1159.
[28] B.Z. Momeni, M.M. Amini, T. Pape, F.E. Hahn, S.W. Ng, Four- and five-coordinate platinum in tris[chlorotris(dimethyl sulfide)platinum(II)] pentakis(trichlorostannyl)-platinate(II) from an $SnCl_2$ insertion into a Pt-Cl bond, J. Mol. Struct. 697 (2004) 97–100.
[29] B.Z. Momeni, L. Jalili Baleh, S. Hamzeh, F. Rominger, Insertion of $SnCl_2$ into Pt-Cl bonds: synthesis and characterization of four- and five-coordinate trichlorostannylplatinum(II) complexes, J. Coord. Chem. 60 (2007) 285–293.
[30] B.Z. Momeni, Z. Moradi, L. Dianati, K. Shahverdi, Studies of the reactions of platinum halo complexes with tin(II) halides, J. Coord. Chem. 62 (2009) 465–474.
[31] B.Z. Momeni, Z. Moradi, M. Rashidi, F. Rominger, Insertion of tin(II) bromide into Pt-X (X = Cl, Br) bond of dimethylplatinum(IV) complexes: a novel polymorphic form of [$PtBr_2$(bpy)], Polyhedron 28 (2009) 381–385.
[32] B.Z. Momeni, H. Kazmi, A. Najafi, Tin(II) halide insertion or halogen exchange in the reactions of dihaloplatinum(II) complexes with tin(II) halide, Helv. Chim. Acta 94 (2011) 1618–1627.
[33] C.J. Levy, R.J. Puddephatt, Energy profile of a rapid, reversible oxidative addition reaction, J. Chem. Soc., Chem. Commun. (1995) 2115–2116.
[34] C.J. Levy, R.J. Puddephatt, Rapid reversible oxidative addition of group 14-halide bonds to platinum(II): rates, equilibria, and bond energies, J. Am. Chem. Soc. 119 (1997) 10127–10136.
[35] C.J. Levy, J.J. Vittal, R.J. Puddephatt, Cationic group 14-platinum(IV) complexes, Organometallics 15 (1996) 35–42.
[36] B.Z. Momeni, S. Eatezadi, Pt-Me bond cleavage in the reactions of dimethylplatinum(II) complexes containing chelating phosphine ligands with organotin(IV) chlorides, Can. J. Chem. 91 (2013) 1288–1291.
[37] B.Z. Momeni, F. Rominger, S.S. Hosseini, Tetrachlorido(1,10-phenanthroline-

κ^2N,N')tin(IV) 1,2-dichloroethane hemisolvate, Acta Crystallogr. E65 (2009) m690.
[38] C.J. Levy, R.J. Puddephatt, Thermal decomposition of platinum(IV)-silicon, -germanium, and -tin complexes, Organometallics 16 (1997) 4115–4120.
[39] S. Achar, J.D. Scott, J.J. Vittal, R.J. Puddephatt, Organoplatinum(IV) polymers and model complexes by oxidative addition of bromoacetate esters, Organometallics 12 (1993) 4592–4598.
[40] P.K. Monaghan, R.J. Puddephatt, Oxidation of dimethylplatinum(II) complexes with alcohols: synthesis and characterization of alkoxoplatinum(IV) complexes, Organometallics 3 (1984) 444–449.
[41] K. Thorshaug, I. Fjeldahl, C. Rømming, M. Tilset, Synthesis, characterization, and acid-base properties of (N-N)$Pt^{IV}(CH_3)_2(OH)_{2-x}(OCH_3)_x$ ($x = 0, 1$) complexes, Dalton Trans. (2003) 4051–4056.
[42] Y.M. Chow, The crystal structure of dimethyltin diisothiocyanate, Inorg. Chem. 9 (1970) 794–796.
[43] D. Seyferth, E.G. Rochow, The reaction of organotin halides with diazomethane, J. Am. Chem. Soc. 77 (1955) 1302–1304.
[44] CrysAlis CCD and CrysAlis RED program, Ver. 171.32.6, Oxford Diffraction Poland, Wrocław, Poland, 2006.
[45] G.M. Sheldrick, A short history of SHELX, Acta Crystallogr. A64 (2008) 112–122.
[46] R.H. Hill, R.J. Puddephatt, A mechanistic study of the photochemically initiated oxidative addition of isopropyl iodide to dimethyl(1,10-phenanthroline) platinum(II), J. Am. Chem. Soc. 107 (1985) 1218–1225.
[47] S. Achar, V.J. Catalano, A search for the elusive red form in substituted Pt^{II} bipyridine complexes, Polyhedron 16 (1997) 1555–1561.
[48] R.H. Herber, M. Croft, M.J. Coyer, B. Bilash, A. Sahiner, Origin of polychromism of *cis* square-planar platinum(II) complexes: comparison of two forms of [Pt(2,2′-bpy)$(Cl)_2$], Inorg. Chem. 33 (1994) 2422–2426.
[49] R.S. Osborn, D. Rogers, Crystal structure of the red Form of 2,2'-bipyridyldichloroplatinum(II), J. Chem. Soc., Dalton Trans. (1974) 1002–1004.
[50] C.R. Barone, L. Maresca, G. Natile, C. Pacifico, A new polymorph of dichlorido(1,10- phenanthroline)platinum(II), Inorg. Chim. Acta. 366 (2011) 384–387.
[51] V. Maheshwari, M. Carlone, F.R. Fronczek, L.G. Marzilli, Ligand and coordination-plane distortions in platinum(II) complexes of isomers of dimethyl-2,2′-bipyridine, Acta Crystallogr. B63 (2007) 603–611.